Sustainable Materials and Technologies 43 (2025) e01221

Contents lists available at ScienceDirect

Sustainable Materials and Technologies

journal homepage: www.elsevier.com/locate/susmat

Upcycling leather waste: The effect of leather type and aspect ratio on the performance of thermoplastic polyurethane composites

Muhammad Umar Nazir [a], Rosario Mascolo [b], Phil Bouic [c], Mohammad Mahbubul Hassan [d], Jane Harris [d], Sara Naderizadeh [a], James J.C. Busfield [a], Han Zhang [a], Dimitrios Papageorgiou [a], Emiliano Bilotti [e,*]

[a] School of Engineering and Materials Science, Queen Mary University of London, London E1 4NS, UK
[b] Stazione Sperimentale per l'Industria delle Pelli e delle Materie Concianti srl, via Campi Flegrei 34, 84134 Pozzuoli, Napoli, Italy
[c] GenPhoenix Ltd., Forli Strada, Alwalton Hill, PE7 3HH Peterborough, UK
[d] Fashion, Textiles and Technology Institute (FTTI), University of the Arts London, 105 Carpenter's Road, London E20 2AR, UK
[e] Department of Aeronautics, Imperial College London, Exhibition Road, London SW7 2AZ, UK

ARTICLE INFO

Keywords:
Leather waste
Tanning
Polymer composites
Average particle size
Aspect ratio

ABSTRACT

Leather is among the most traded commodities globally, despite being one of the most ancient engineered natural materials and a by-product of the meat industry. This reflects its high perceived commercial value as well as its unique physical properties such as tear and wear resistance, thermal stability, and breathability. However, transforming animal hide into leather is a complex process that faces several process issues that could impact the environment. Moreover, the low yield of final leather products, combined with the lack of viable end-of-life options, has drawn significant attention from the research community. Herein, we systematically explore the potential for upcycling leather waste by incorporating it into thermoplastic polyurethane (TPU). TPU composites with various contents of leather waste (5 to 30 wt%), sourced from different tanning methods and with different particle size distributions, were prepared by melt compounding and studied for their morphological, thermal, and mechanical properties as well as tear and abrasion resistance. This work demonstrated that enhanced mechanical properties (Young's modulus 305 MPa) and abrasion resistance are significantly influenced by the average particle size of the leather waste, with the highest aspect ratio (61) of wet blue leather providing the best performance.

1. Introduction

The transformation of skins and hides into suitable artefacts is one of the oldest technologies in human history. Still, the market capitalisation of leather will reach US$ 405.28 billion by 2030 with a compound annual growth rate of 6.6 % [1,2]. A series of chemical and physical treatments are necessary to transform a raw hide into leather. The process of tanning, in particular, is considered the turning point in stabilising a putrescible biological material, making it capable of withstanding further processing and enhancing organoleptic properties [3].

Skin is primarily composed of collagen, a polar protein and a generic name for a family comprising at least 28 different types of collagens, among which collagen Type I is the most important and copious [3,4]. Morphologically, skin shows a layered interwoven fibrous structure, with a fine top (grain) and coarse bottom (corium) layer. The fine grain layer imparts strength and smoothness whereas the coarse corium layer improves toughness and tear resistance [5–8]. This combination makes leather a versatile material that has served human beings for ages, ranging from footwear to the built environment and vehicle interiors.

Nevertheless, leather manufacturing is very inefficient and involves many chamicals with potential risks on the environment like heavy metals used in tanning and retanning processes [9–12]. Tanning is the transformative step during leather manufacturing and is carried out using different substances, including chromium salts, glutaraldehyde, or vegetable tannins, producing leathers often referred to as wet blue, wet white, or vegetable-tanned, respectively.

Leather waste comes in different forms, mainly including non-tanned and tanned solid waste and fleshing waste, accounting for approximately 80 % of the original hide or skin, leaving a meagre yield of 20 % [13,14]. The great amount of waste determines consequent problems in

* Corresponding author.
E-mail address: e.bilotti@imperial.ac.uk (E. Bilotti).

https://doi.org/10.1016/j.susmat.2024.e01221
Received 19 April 2024; Received in revised form 6 September 2024; Accepted 14 December 2024
Available online 16 December 2024

the disposal as traditional methods of waste management like landfilling and incineration are becoming unacceptable. Site limitations, higher transportation costs, chromium leachate, and release of methane gas restrict landfilling. Incineration of leather waste at elevated temperatures is limited because of chromium conversion from trivalent to hexavalent, which is a genotoxic carcinogen [15,16]. Therefore, it is necessary to develop novel applications for leather waste to mitigate their disposal issues.

The significant environmental challenge posed by leather waste has led the research community to investigate innovative and more sustainable solutions. Several studies have been conducted from this perspective, including the use of leather waste as animal feed or biofertilisers [17,18], as adsorbents [19], carbon dots [20], for the extraction of collagen and chromium [21–23], as reconstituted collagen, and as filler in polymer composites [24–26].

With regard to polymer composites, leather waste has been incorporated into various polymer matrices including epoxy [27], high-density polyethylene [28], natural rubber [29,30] [31,32], unsaturated polyester [33], thermoplastic polyurethane [25], polyvinyl alcohol [34], and polylactic acid [35]. These results revealed some interesting insights in terms of mechanical properties. Li et al. demonstrated an increase in tensile strength and toughness of natural rubber by almost 30 % and 60 %, respectively, with the addition of 5 % of silane-modified leather collagen fibres [36]. Similarly, the addition of 5 parts by weight of leather buffing dust as a filler into carboxylate butadiene-acrylonitrile rubber improved the tensile strength from 8.51 to 14.88 MPa along with increased resistance to thermal ageing [37].

In this research, thermoplastic polyurethane (TPU) was selected as the polymer matrix to develop leather waste composites, as it resembles the chemistry of most leather finish and faux leathers. TPU is an interesting class of linear block elastomeric copolymers that exhibits desirable features such as abrasion resistance, large reversible elastic deformations, and adhesion to many substrates, combined with potential recyclability via simple thermomechanical methods [38–40]. Surprisingly, only a few studies have been reported so far on TPU-based leather waste composites. Li et al. investigated the mechanical properties and morphology of TPU/leather composites and reported a considerable improvement in the toughness of these composites, from 3.4 to 61.8 MJ/m^3, after using binary solvents (*N*, *N*-dimethylformamide, and toluene) to disperse 5 to 25 % of leather powder, but still considerably lower than the toughness of pure TPU [25]. In another attempt, Liu et al. investigated the mechanical properties of TPU/leather composites after defibrillating the leather fibres through different milling cycles. They achieved a slight increase in terms of tensile strength, from 9 MPa to 14.5 MPa, after vigorous milling of leather [41]. In both these attempts, the focus was on the surface modification and defibrillation of a single type of leather, to improve, respectively, toughness or tensile strength.

This is particularly significant because the properties of composites are highly dependent on the reinforcement materials, such as their mechanical properties (Young's modulus). However, the influence of the type of leather and the average particle size of recycled leather fibres on the properties of polymer composites, especially TPU/leather composites, has not been systematically investigated. In this study, we show that the mechanical properties of polymer/leather composites can be substantially improved by employing leather fibres with a high aspect ratio, a finding that aligns with predictions from the Halpin-Tsai micromechanical analytical model.

2. Materials and method

2.1. Materials and composites preparation

Leather wastes of different types were kindly provided by GenPhoenix Ltd. (UK) and SSIP (Stazione Sperimentale per l'Industria delle Pelli e delle Materie Concianti) (Italy), as milled fibrous powders. These wastes included wet blue (GenPhoenix), wet white (SSIP), and vegetable-tanned (SSIP) leather, covering the most common tanning methods used industrially. A reference finished leather (a chromium-tanned bovine leather product) was provided by Eako Limited. The thermoplastic polyurethane used was Estane 58,437, from Lubrizol (USA). Ethanol was purchased from Sigma Aldrich. TPU pellets and all types of leather fibres were subjected to overnight drying at 80 °C before further use. Leather wastes were incorporated into the TPU matrix via melt compounding, at leather contents of 5 %, 10 %, 20 %, and 30 % by weight, with an Xplore MC15 HT Micro Compounder, at 180 °C and 100 rpm for 2 min. Specimens for the following tests were prepared by compression moulding, using a Hot Press 3100 (Dr Collins, Germany), at 180 °C and 100 bar for 2 min, followed by cooling to room temperature under pressure for about 5 min.

2.2. Optical microscopy

A small amount of leather fibres (0.03 g) was added to ethanol (30 mL), vigorously shaken, and cast dropwise onto a glass cover slide. After ethanol evaporated at ambient conditions, the leather particles on the cover slides were statistically analysed (at least 100 particles measured for each leather type) for their size distribution, using the optical microscope TR 300 (VWR International Belgium) with a lens magnification of 4×.

2.3. Scanning Electron microscopy

The cross-sectional areas of the specimens, cold fractured after immersion in liquid nitrogen, were analysed using an Inspect F Scanning Electron Microscope (SEM) by FEI Thermo Fisher Scientific, to reveal the leather fibre dispersion in the TPU matrix. The micrographs were taken at 5 kV and a magnification range of 70× and 40,000×. Before scanning, the specimens were coated with a 10 nm gold layer using an automatic sputter coater by Agar Scientific to induce electroconductivity and avoid artefacts caused by local charging.

2.4. FTIR spectroscopy

Fourier Transform Infra-Red (FTIR) spectroscopy of different leather fibres was carried out using a Bruker Tensor 27 Spectrometer with ATR assembly. A transmittance spectrum of 48 scans was collected over a range from 400 to 4000 cm^{-1} with a resolution of 4 cm^{-1}.

2.5. Thermal analysis

Thermal Gravimetric Analysis (TGA) and Differential Scanning Calorimetry (DSC) of TPU, leather fibres, and their composites were carried out to identify any thermal decomposition and phase transition. TGA was carried out with a TA Instrument TGA 5500, heating from room temperature to 800 °C at a rate of 20 °C per minute, under a nitrogen atmosphere. DSC was carried out with a TA Instruments DSC 25, using heating/cooling cycles between −80 °C and 250 °C, at a rate of 20 °C per minute, under a nitrogen atmosphere.

2.6. Mechanical testing

Tensile testing was carried out on dog-bone-shaped specimens, in accordance with type V of the ASTM standard D638, using an Instron 5967 equipped with a load cell of 1 kN. The composite specimens were mounted on the Instron machine using pneumatic grips at a constant pressure of 6 bar. The Young's modulus was calculated in the linear elastic region, between 0.05 % and 0.25 % strain (at a crosshead speed of 1.0 mm/min). At least five specimens of each composition were tested, and average values were reported.

Tear testing was carried out on rectangular specimens of 0.4 mm thickness, 25 mm width and 70 mm length, according to the standard

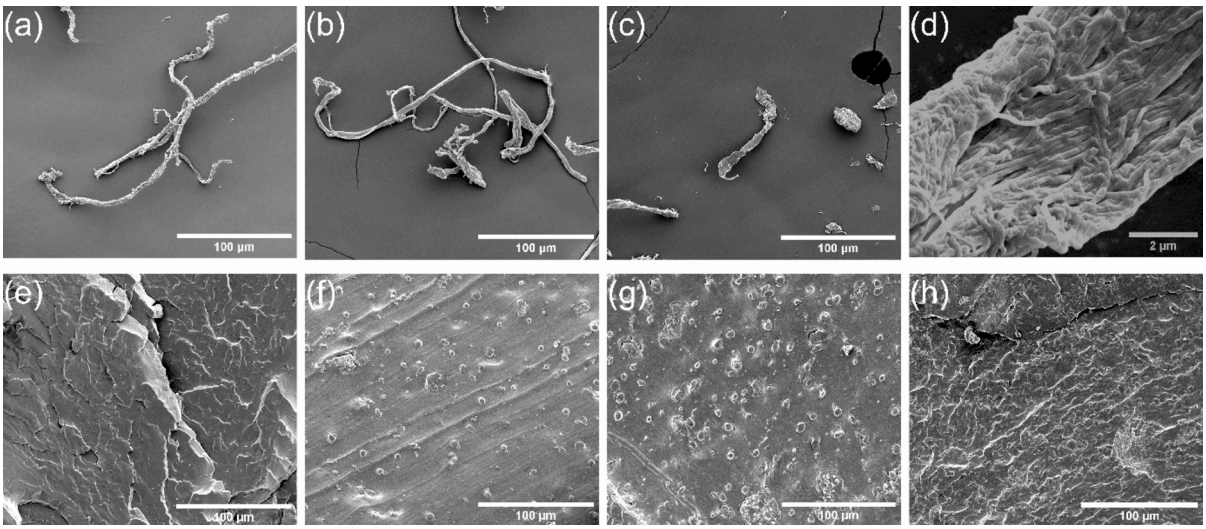

Fig. 1. SEM micrographs of different leather waste fibres and TPU/VEG composites. a) Wet Blue. b) Wet White. c) VEG fibres. d) Collagen fibril bundles within VEG. Cryo-fractured e) TPU, f) TPU/VEG 10, g) TPU/VEG 20, and h) TPU/VEG 30.

ASTM 1938–19, using an Instron 5967 equipped with a 1 kN load cell, at a crosshead speed of 250 mm/min. At least four specimens of each composition were tested, and average values were reported.

The abrasion resistance of the composites was determined using a Rotating Cylindrical Drum following the ISO Test Method 4649:2017, on circular specimens of 16 mm diameter and 5 mm thickness. At least three specimens of each composition were tested, and average values were reported.

2.7. Halpin Tsai model

Halpin-Tsai is a semi-empirical method often used to predict the mechanical properties of discontinuous short-fibre reinforced composites. This model was used to estimate the Young's Modulus of the TPU/leather composites (Ec, Eq. (1)), once the moduli of the polymer matrix (E_m) and filler (E_f) are known, as well as the volume fraction (v_f), orientation factor (a), the filler aspect ratio (l/d), and the coefficients η_L (Eq. (3)) and η_T (Eq. (5)). E_L and E_T are the estimated Young's Moduli of the composites along the fibre direction or transverse to it. If the aspect ratio becomes infinitely large the Halpin Tsai model reduces to the parallel model and if the aspect ratio becomes 1, the Halpin Tsai model reduces to the series model. The prediction curves of these parallel and series models are presented in Fig. S4 (c, d) in the supplementary information for further explanation and understanding.

$$E_c = aE_L + (1-a)E_T \tag{1}$$

$$E_L = E_m \frac{1 + \frac{l}{d}\eta_L v_f}{1 - \eta_L v_f} \tag{2}$$

$$\eta_L = \frac{\frac{E_f}{E_m} - 1}{\frac{E_f}{E_m} + \frac{l}{d}} \tag{3}$$

$$E_T = E_m \frac{1 + 2\eta_T v_f}{1 - \eta_T v_f} \tag{4}$$

$$\eta_T = \frac{\frac{E_f}{E_m} - 1}{\frac{E_f}{E_m} + 2} \tag{5}$$

$$E_c = E_m v_m + E_f v_f \tag{6}$$

$$E_c = \frac{E_f E_m}{E_f v_m + E_m v_f} \tag{7}$$

3. Results and discussion

3.1. Morphological studies

All the leather wastes analysed appeared as fibrous material. Fig. 1.a-c shows the typical morphology of these fibres. Each fibre presents a hierarchical structure, formed by the assembly of collagen fibril bundles visible in Fig. 1.d. The chemical nature of such fibres is confirmed by FTIR spectra (Fig. S1, in SI, and Fig. 3.a), showing characteristic amide peaks of collagen [42,43].

The average aspect ratio of the leather fibres was calculated from the ratio of the largest dimension (i.e. length) and the smallest dimension (i.e. diameter) and reported in Table S1. Wet blue possessed the largest aspect ratio (61) combined with the smallest fibre diameter (13 μm). Wet white and vegetable-tanned leather fibres showed a similar length to that of WB leather fibres but a larger diameter, resulting in about 1/3 of WB fibres' aspect ratio.

Figs. 1f-h show the cross-sectional areas of the TPU composites containing different amounts of vegetable-tanned leather waste, compared with pure TPU (Figs. 1e). TPU composites containing WW and WB present a similar morphology and are included in Fig. S2 in the SI. Leather particles are rather homogeneously dispersed in the TPU matrix for filler content up to 20 wt%. The fibrous leather particles appear well adhered to the TPU matrix, with no signs of fibre pullout. For the highest filler contents (i.e. 30 wt%), the composites presented some evidence of filler agglomeration, with an expected negative influence on the final mechanical properties. At such high filler content, some cavities are also visible (Figs. S2.a-h), probably caused by the detachment of larger leather agglomerates, which were not sufficiently well embedded in the polymeric matrix.

3.2. Thermal analysis

The DSC thermogram of pure TPU in Fig. 2.a shows three main features: two glass transition temperatures, at −34 °C and 14 °C, related to soft and hard segments of the TPU, respectively [44,45], and a small endothermic peak at 182 °C, attributed to a slight degree of crystallinity, most probably within the hard segment region of TPU [46].

When leather of different types and contents was added to the TPU,

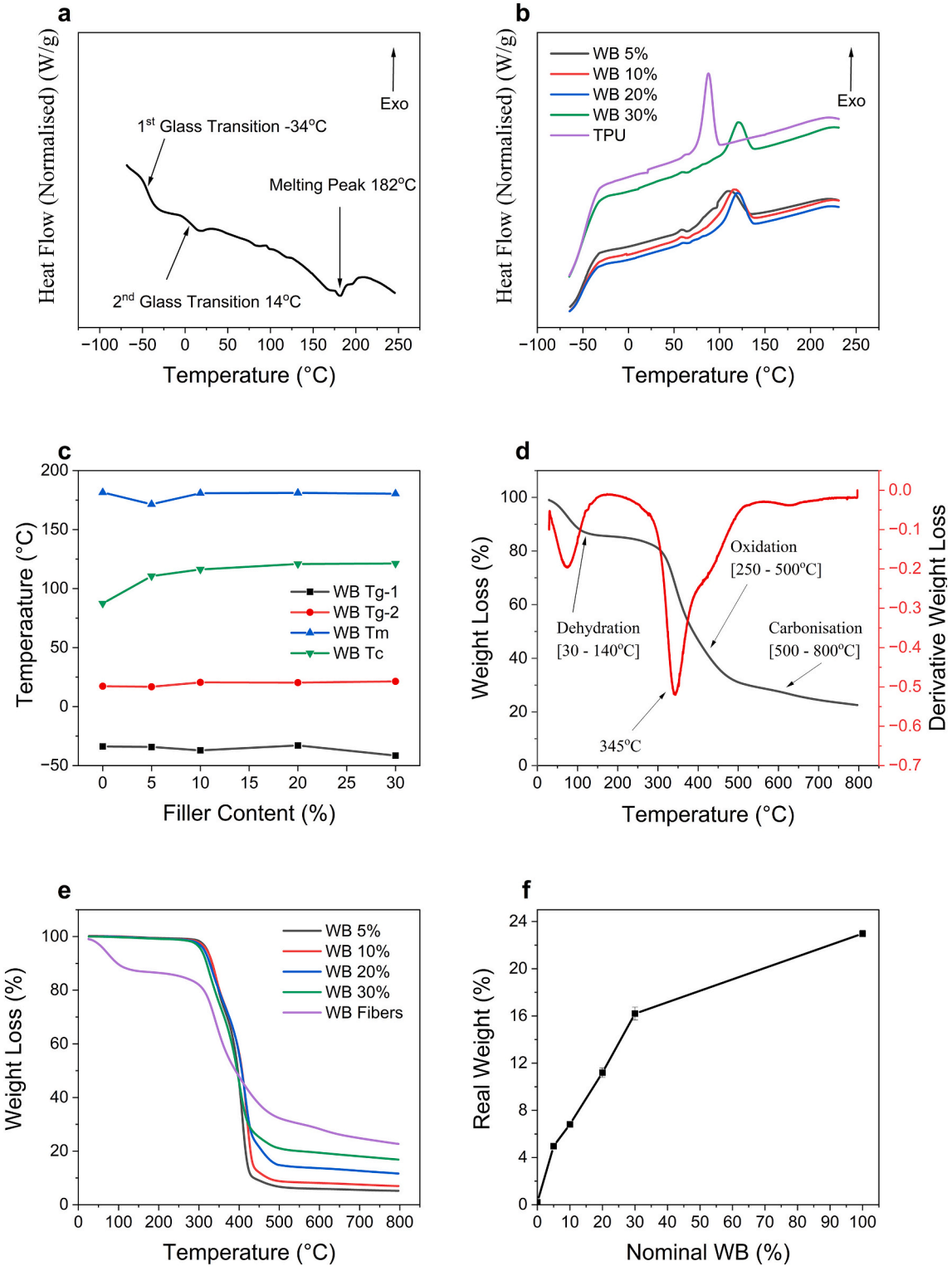

Fig. 2. DSC and TGA curves of TPU and its composites: a) DSC second heating curves; b) DSC cooling curves; c) effect if WB fibre filler loading on the crystallisation, melting and glass transition temperatures of TPU/WB composites; d) TGA/DTG curves of WB fibres; e) TGA curves of TPU/WB leather composites and f) their residual ash contents at 800 °C.

no significant change in the two glass transition temperatures and the melting temperature was observed (Fig. 2.c). However, the addition of small amounts (<10 wt%) of wet blue leather caused a significant shift in the crystallisation temperature of TPU (from 88 °C to 116 °C), which suggests a nucleating effect of leather (Fig. 2.b-c) [47]. However, the comparison of exothermic peaks of neat TPU and its composites highlights an increase in the peak broadness for the composites (Fig. 2b), which might be explained by the presence of less perfect polymer crystals.

The thermogravimetric curves of TPU [48], wet blue leather, and their composites [22,27], are illustrated in Fig. S3.a-c and Figs. 2d-2f, respectively. In nitrogen, the decomposition of TPU started at 290 °C,

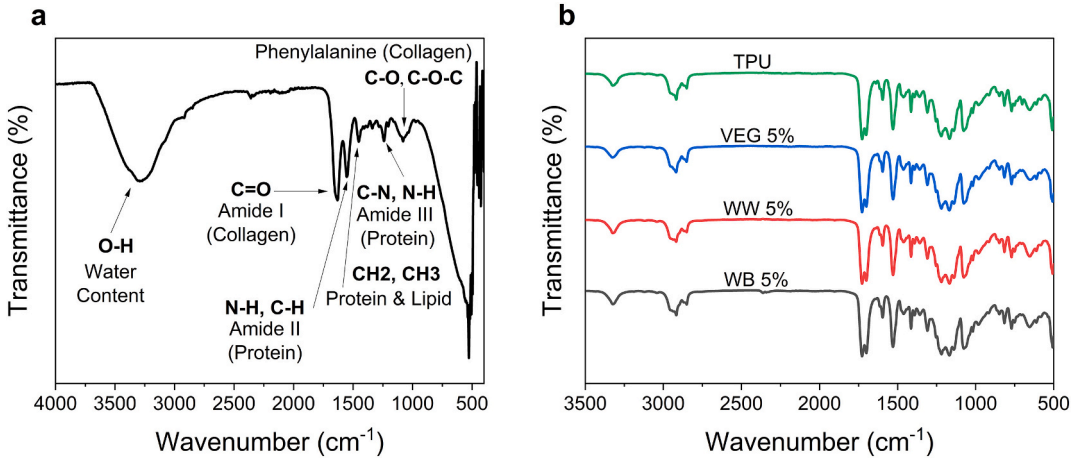

Fig. 3. a) FTIR of WB leather waste fibres, b) ATR-FTIR spectra of thermally processed TPU and its composites with various types of leather waste particles.

with a main degradation peak at 400 °C after a shoulder peak at 350 °C (Fig. S3.a). The shoulder degradation peak is attributed to the dissociation of urethane groups, followed by the formation of diols, diisocyanates, and the release of CO_2 [49]. The main decomposition peak is attributed to the decomposition of the soft segment of the TPU matrix, leading to the formation of a complex mixture of molecular species derived from the fragmentation of polyol segments. After 600 °C no solid residue was detectable [50].

Wet blue leather waste revealed three distinct decomposition steps [51] during TGA analysis in nitrogen (Fig. 2d). The first decomposition step, between 30 °C and 140 °C, is due to dehydration of leather. Naturally, leather is hygroscopic, typically containing 15–30 % moisture, depending upon the surrounding environmental conditions and treatment [52–54]. The second degradation step, between 300 °C and 500 °C, with a peak at 345 °C, is ascribed to the decomposition of the core collagen material [55]. The last degradation step, relatively smaller than the previous two, appeared at temperatures between 500 °C and 800 °C. This last degradation step can be explained by carbonization, leaving a solid residue of 15–25 % [56]. The residual ash content at the end of decomposition was higher for vegetable-tanned leather (Fig. S3b-S3c), consistent with published literature, probably due to the presence of natural phenolic compounds [57,58]. The decomposition curves and the solid residue at 800 °C, relative to all compositions of WB, are presented in Figs. 2.e-f. The solid residue curves can be used as a verification of the nominal filler content added during melt compounding, once calibrated for the degradation of pure TPU and the three leather waste fibres.

3.3. FTIR spectral analysis

Fig. 3.a (and Fig. S1b, in SI) presents the FTIR spectrum of a WB leather sample, which shows typical collagen biopolymer-associated amide (III), amide (II) and amide (I) IR bands at 1234, 1535, and 1650 cm^{-1}, respectively. The broad IR band observed at 3323 cm^{-1} is associated with the hydroxyl groups of collagen. The IR band at 1031 cm^{-1} is associated with C-O-C and C—O groups of collagen. The FTIR spectrum of WB leather fibre is similar to the spectrum of the leather sample shown in Fig. S1, with the same IR bands, but with a slight change in intensity and position, suggesting the formation of ionic or hydrogen bonding. This occurs due to the breakage and the rearrangement of the hydrogen bonding in leather waste fibres under the strong shearing and compression during grinding for their extraction process. In the case WB, collagen macromolecules are bonded together by ionic crosslinking with trivalent chromium ions, considerably increasing their tensile strength and decreasing elongation. In the case of WW and VEG-tanned leather, new sharp bands are present at 1006 cm^{-1} associated with sulphonate moieties, which are absent in the spectrum of WB-tanned leather sample particles, suggesting that these two leather samples were treated with sulphonated syntans. In the case of WW, the collagen fibrils are covalently crosslinked together by glutaraldehyde, while for VEG-tanned leather, they are crosslinked with natural tannins, which mostly form hydrogen bonding [59]. However, glutaraldehyde is not ionic and thus it is difficult to diffuse into collagen fibrils, partially compromising the final performance compared to the Cr-tanned leather.

Fig. 3.b shows the ATR-FTIR spectra of processed TPU and TPU/leather particle composites. The spectra of TPU show typical TPU-related IR bands at 557, 1078, 1234, 1332, 1444, 1535, 1630, 2850, 2931 and 3290 cm^{-1}. The IR band at 3290 is associated with the hydrogen-bonded N—H [59]. The IR bands at 2850 and 2931 are associated with the C—H asymmetric and symmetric stretching vibrations in the -CH_2 groups [60,61]. The IR bands at 1444, 1535, and 1630 cm^{-1} are associated with the bending mode of C—H of methyl groups, N—H bending vibration, and conjugated C—C bond of the unsaturated ester, respectively. The composites of TPU with various leather waste fibres also show similar IR bands; TPU-associated bands are overlapping with the hydroxyl, amide (I), amide (II) and amide (III) bands at 3327, 1600, 1529 and 1219 cm^{-1}, respectively. In the case of leather waste particles, these bands were at 3323, 1234, 1535, and 1650 cm^{-1}, respectively (Fig. S1.b). The FTIR spectra of all composites show a new band at 1728 cm^{-1} (which is absent in the spectra of TPU and leather waste particle) that is associated with the ester (C=O), suggesting the formation of an ester bond between the TPU and leather waste particles which causes a considerable increase in tensile strength of the composites compared to the TPU alone [62]. The change in position of these IR bands for TPU/leather waste particle composites suggests the formation of hydrogen bonds between hydroxyl groups of TPU and amino, carboxyl and hydroxyl groups of leather waste particles. The spectra of composites of TPU with all three leather wastes show the same IR bands with similar intensities suggesting that all three leather wastes have similar interactions with TPU.

3.4. Mechanical tensile properties

The physical properties of composite materials are, in general, influenced by their morphological structures, distribution of fillers and bonding between surfaces of filler and the polymer matrix, as discussed in the previous sections. The mechanical properties (Young's modulus, tensile strength, and elongation at break) of TPU/leather composites were investigated under tensile loading and are presented in Fig. 4. The finished leather was also tested using the same protocols for reference purposes. Additionally, various types of finished leather that underwent different tanning techniques were tested for reference purposes, and the

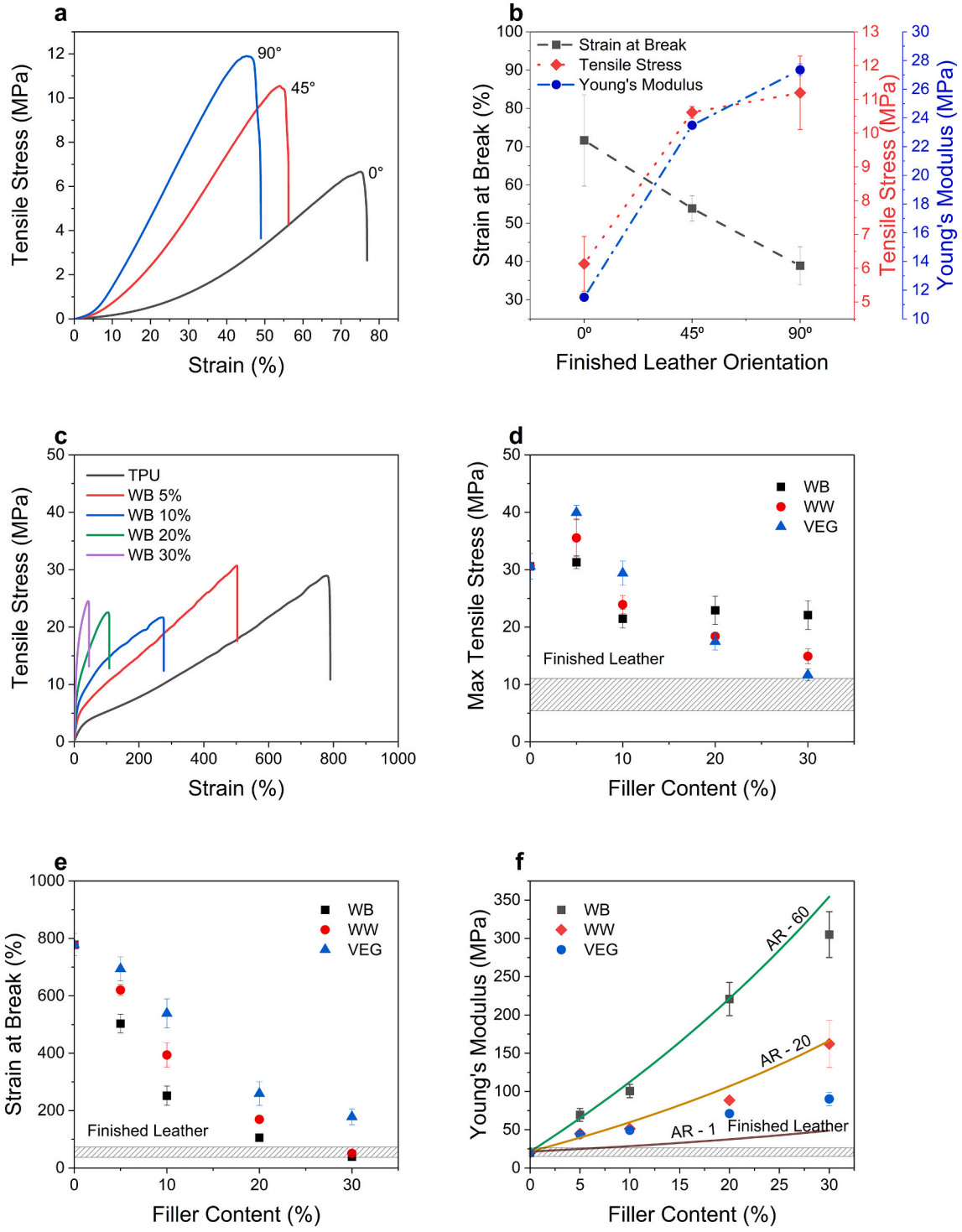

Fig. 4. Mechanical tensile properties of finished leather and TPU/leather waste composites. Tensile stress-strain curves (a) and average values of Young's Modulus, maximum tensile stress and Strain at Break (b) of finished leather, measured along three tilt angles. c) Tensile stress-strain curves of TPU and TPU composites containing different amounts of WB. Average maximum tensile stress (d), strain at break (e) and Young's Modulus (f) of TPU composites containing different amounts of WB, WW and VEG. The values of the average Young's Modulus are fitted with the Halpin-Tsai predictions, for different aspect ratios (AR).

results are presented in Table S2. Finished leather is a fibrous material whose mechanical properties also depend on the orientation of the constituting collagen fibres, which changes throughout the hide, making leather anisotropic. To evaluate the mechanical anisotropy of this finished leather, specimens were cut and tested along three directions (viz 0°, 45° and 90°, where 0° is parallel to the largest side of the rectangular finished leather), as reported in Figs. 4.a-b. TPU and composites with low leather content (up to 5 wt%) exhibited values of Young's modulus and maximum tensile stress similar to the finished leather product but with a higher strain at break. As expected, the strain at break decreased with increasing filler content, until approaching values similar to the finished leather for TPU composites containing 30 wt% of WB, WW, or VEG-tanned leather waste. Among the different types of leather, wet blue achieved the highest values of Young's modulus and

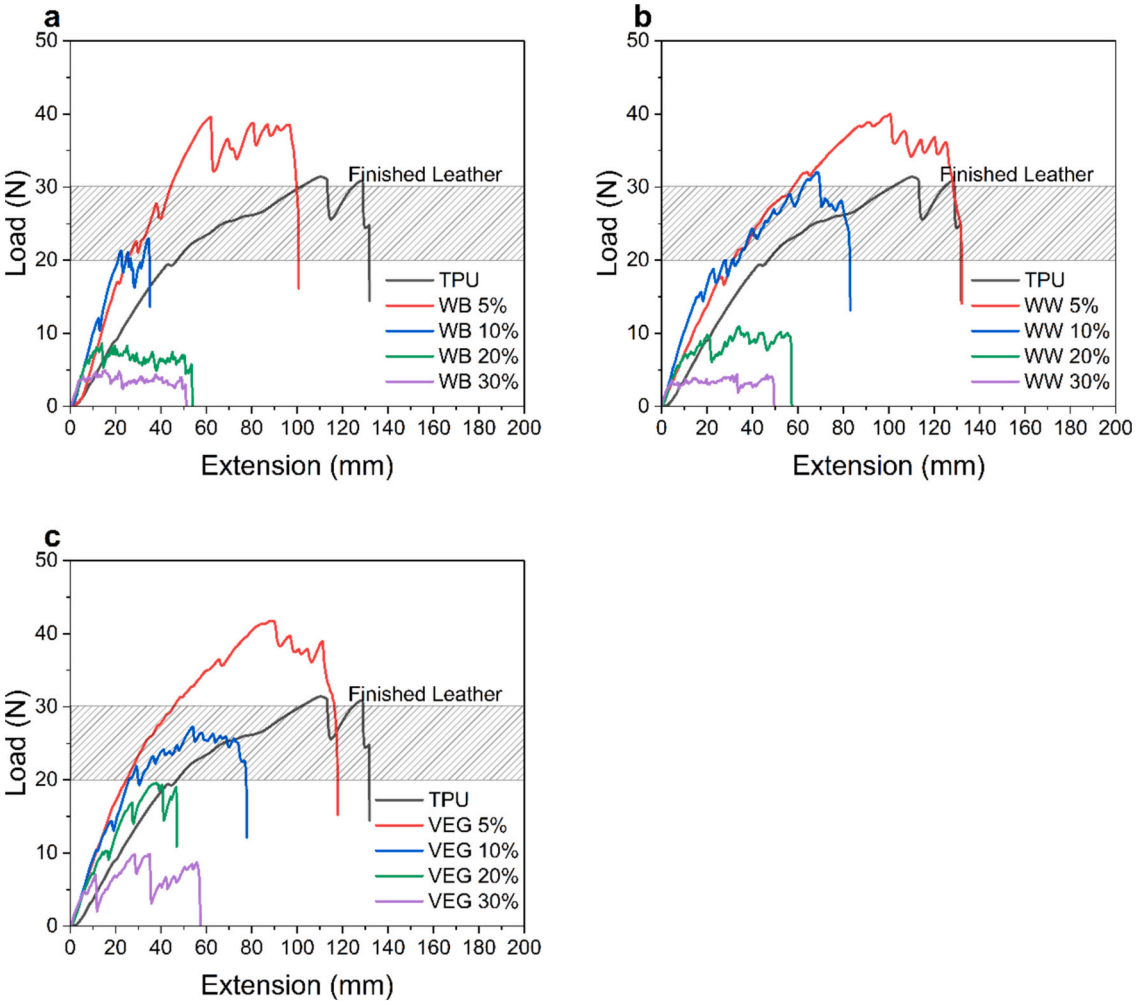

Fig. 5. Tear Propagation Resistance of TPU composites containing different amounts of the three leather wastes.

tensile stress. It is interesting to note that the results of composite stiffness correlated with the values of aspect ratios measured by optical microscopy (Table S1). In particular, higher aspect ratio fillers provided higher Young's moduli, consistent with micromechanical composite theories.

The direct (parallel) and inverse (series) Rule of Mixture (Eqs. (6 & 7)) provide, respectively, the highest and lowest theoretical limits, based on the Young's modulus and the content of the two phases (i.e., TPU polymer matrix and fibrous collagen reinforcement, with a Young's modulus taken as 11.5 GPa) [63–65]), as presented in Fig. S4.c. It can be observed that vegetable-tanned leather-based composites lie close to the lower boundary of the series model, which is valid for particulate fillers. Wet blue leather provides the highest mechanical reinforcement among all leather types, with an aspect ratio of 61, but is still far from the upper boundary given by the parallel model, valid for continuous reinforcing fibres. These observations are in line with Halpin-Tsai predictions, which provide the possibility of a more quantitative analysis (Fig. S4.d). An aspect ratio of 20 (Wet White and Vegetable-tanned leather) is predicted to give a mechanical reinforcement close to the lowest starting plateau. With an aspect ratio of 61, the mechanical reinforcement of Wet Blue leather lies in the intermediate region between the lowest and highest plateau. To reach the highest reinforcement potential, a leather fibre with an aspect ratio exceeding 1000 should be employed. This simple model can, therefore, be used to estimate the leather fibre size necessary for an efficient composite and to provide a guideline value for future leather defibrillation efforts. Assuming a leather fibre length of 1 mm (just slightly longer than our WB, WW, and VEG leather), a fibre diameter of 1 μm should be obtained, which is 40 times smaller than usual values obtained via traditional milling processes but still much larger than the typical collagen fibril bundle diameter (~100-200 nm, Fig. 1.d). This presents a challenge and a sense of direction for the field.

3.5. *Tear strength*

The tear propagation resistance of TPU/leather composite sheets was determined under tear-trouser or single-rip tearing tests and presented in Fig. 5. Interestingly, 5 wt% of WB, WW, and VEG leather fillers increased the average maximum tear load of TPU, from about 30 N to 40 N. This increase could be due to the formation of ester bonds between the TPU and leather waste particles, as demonstrated earlier (Section 3.3). However, a further increase in the leather fillers loading caused a decrease in tear resistance, mainly caused by a decrease in strain at break and increased embrittlement, as shown from tensile tests (Fig. 4.f). Tear testing of the finished leather was carried out in three different directions, viz., 0°, 45°, and 90° (Fig. S5 in SI), and the average values are presented in Fig. 5 as a shaded region. The results demonstrate that the tear propagation values of the finished leather are comparable, in terms of load, with TPU and TPU composites with up to 10 wt% leather waste content. A further increase in tear resistance of the TPU composites with higher waste leather fibre contents can be expected for finer and higher aspect ratio fibres, as well as with the addition of cross-linkers, and perhaps, suitable plasticisers.

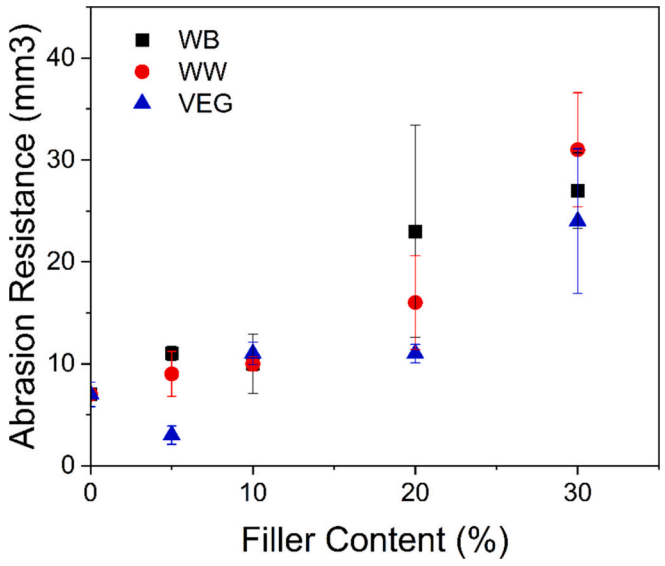

Fig. 6. Abrasion Resistance of TPU composites containing different amounts of the three leather wastes.

3.6. *Abrasion resistance*

The abrasion resistance of leather composites is summarised in Fig. 6. The finished leather was also tested for reference purposes, but did not survive the abrasion test (failed after 5 cycles of abrasion) and was therefore assigned with a value of zero. The addition of leather fillers monotonically improves the abrasion resistance of TPU. Despite a large scattering of data, the wet blue and wet white leather fibre composites demonstrated a better abrasion resistance than the other composites, showing a twofold increase in abrasion resistance associated with the larger aspect ratio of the fillers. A higher aspect ratio contributed to a higher Young's modulus, a higher orientation of these fillers, and a better distribution of the abrasive forces which ultimately resulted in improved the abrasion resistance of these composites.

4. Conclusion

In this work, different types of leather waste fibrous materials, with average aspect ratios between 20 and 61, were upcycled into TPU/leather composites via a simple melt compounding process. SEM morphological analysis revealed a good dispersion of leather fibres in the TPU matrix and effective interfacial adhesion between the thermoplastic elastomer and leather fibres, which rendered any surface functionalization redundant. Only at the highest leather contents studied (30 wt%), did the composites exhibited agglomeration of leather fibres, which had a negative effect on the ductility of the composites. Overall, the addition of leather waste fibres increased Young's modulus and abrasion resistance of TPU across all filler contents and improved the maximum tensile stress and tear resistance for leather contents less than 10 % surpassing the values for a finished leather product.

The aspect ratio of the leather waste fibres was found to directly correlate with the mechanical properties of the resultant composites, with wet blue leather (aspect ratio of 61) providing a higher mechanical reinforcement, compared to wet white and vegetable-tanned leather fibres (aspect ratio of 20). Using the Halpin-Tsai micromechanical model, it was estimated that an aspect ratio exceeding 1000 should be employed to achieve the highest theoretical mechanical properties. Developing a simple and scalable method to obtain leather fibres with diameters around 1 μm or below could result in the viable upcycling of leather waste into different consumer and engineering products.

CRediT authorship contribution statement

Muhammad Umar Nazir: Writing – original draft. **Rosario Mascolo:** Writing – review & editing, Resources. **Phil Bouic:** Writing – review & editing, Resources. **Mohammad Mahbubul Hassan:** Writing – review & editing, Writing – original draft. **Jane Harris:** Writing – review & editing. **Sara Naderizadeh:** Writing – review & editing. **James J.C. Busfield:** Writing – review & editing. **Han Zhang:** Writing – review & editing, Supervision. **Dimitrios Papageorgiou:** Writing – review & editing, Supervision. **Emiliano Bilotti:** Writing – review & editing, Supervision, Conceptualization.

Declaration of competing interest

None.

Acknowledgement

Muhammad Umar Nazir is a PhD researcher who is partially funded by Higher Education Commission of Pakistan. The authors thank Eako Limited for their donation of the finished leather. The Arts and Humanities Research Council of the UK (AH/S002804/1) is also acknowledged for its partial financial support.

Appendix A. Supplementary data

Supplementary data to this article can be found online at https://doi.org/10.1016/j.susmat.2024.e01221.

Data availability

Data will be made available on request.

References

[1] M.M. Hassan, J. Harris, J.J.C. Busfield, E. Bilotti, A review of the green chemistry approaches to leather tanning in imparting sustainable leather manufacturing, Green Chem. (2023), https://doi.org/10.1039/D3GC02948D.
[2] Grand View Research, Electronic PDF [Online]. Available: https://www.grandviewresearch.com/press-release/global-leather-goods-market, 2024.
[3] A.D. Covington, Modern tanning chemistry, Chem. Soc. Rev. (1997) 111–126.
[4] A.D. Covington, W.R. Wise, Collagen and skin structure, in: Tanning Chemistry: The Science of Leather, 2023, pp. 1–31, https://doi.org/10.1039/9781788012041-00001.
[5] I. It, "Skin and its Components 2.1," no. Chapter 5, 2009.
[6] D.N. O'leary, G.E. Attenburrow, Differences in strength between the grain and corium layers of leather, J. Mater. Sci. 31 (1996) 5677–5682.
[7] B.M. Haines, J.R. Barlow, The anatomy of leather, J. Mater. Sci. 10 (1975) 525–538.
[8] S.J.R. Kelly, et al., Effect of collagen packing and moisture content on leather stiffness, J. Mech. Behav. Biomed. Mater. 90 (2019) 1–10, https://doi.org/10.1016/J.JMBBM.2018.10.004.
[9] C. Bini, L. Maleci, A. Romanin, The chromium issue in soils of the leather tannery district in Italy, J. Geochem. Explor. 96 (2–3) (2008) 194–202, https://doi.org/10.1016/j.gexplo.2007.03.008.
[10] B.R. Eastman, et al., The effectiveness of vermiculture in human pathogen reduction for USEPA biosolids stabilization, Compost Sci. Util. 9 (1) (2001) 38–49, https://doi.org/10.1080/1065657X.2001.10702015.
[11] F. Langmaier, P. Mokrejs, K. Kolomazník, M. Mládek, R. Karnas, Cross-linking epoxide resins with hydrolysates of chrome-tanned leather waste, J. Therm. Anal. Calorim. 88 (3) (2007) 857–862, https://doi.org/10.1007/s10973-005-7458-1.
[12] B. Dhal, H.N. Thatoi, N.N. Das, B.D. Pandey, Chemical and microbial remediation of hexavalent chromium from contaminated soil and mining/metallurgical solid waste: a review, J. Hazard. Mater. 250–251 (2013) 272–291, https://doi.org/10.1016/j.jhazmat.2013.01.048.
[13] S. Hüffer, T. Taeger, Sustainable leather manufacturing - a topic with growing importance, J. Am. Leather Chem. Assoc. 99 (10) (Oct. 2004) 424–428.
[14] S.K. Verma, P.C. Sharma, Current trends in solid tannery waste management, Crit. Rev. Biotechnol. 43 (5) (2022) 805–822, https://doi.org/10.1080/07388551.2022.2068996.
[15] M. Velusamy, B. Chakali, S. Ganesan, F. Tinwala, S. Shanmugham Venkatachalam, Investigation on pyrolysis and incineration of chrome-tanned solid waste from tanneries for effective treatment and disposal: an experimental study, Environ. Sci. Pollut. Res. 27 (24) (Aug. 2020) 29778–29790, https://doi.org/10.1007/S11356-019-07025-6/TABLES/4.

[16] C. A. & W. T. F. Jr. M. E. Losi, Environmental biochemistry of chromium, in: Rev. Environ. Contam. Toxicol, 1994, pp. 91–121.
[17] Rubina Chaudhary, Anupama Pati, Purification of protein hydrolyzate recovered from chrome tanned leather shaving waste, J. Am. Leather Chem. Assoc. 111 (1) (2016) 10–16 [Online]. Available: https://www.scopus.com/record/display.uri?eid=2-s2.0-84960112421&origin=resultslist.
[18] R. Chaudhary, A. Pati, Poultry feed based on protein hydrolysate derived from chrome-tanned leather solid waste: creating value from waste, Environ. Sci. Pollut. Res. 23 (8) (2016) 8120–8124, https://doi.org/10.1007/s11356-016-6302-4.
[19] J.S. Tahiri, M. Azzi, A. Messaoudi, A. Albizane, M. Bouhria, S. Alami Younssi, Mabrour, Removal of methylene blue from aqueous solutions by adsorption on tanned solid wastes, J. American Leather Chemi. Assoc. 97 (7) (2024) 261–266.
[20] W. Zhang, et al., Turning waste into treasure: multicolor carbon dots synthesized from waste leather scrap and their application in anti-counterfeiting, ACS Sustain. Chem. Eng. 11 (13) (Apr. 2023) 5082–5092, https://doi.org/10.1021/ACSSUSCHEMENG.2C07045/ASSET/IMAGES/LARGE/SC2C07045_0011.JPEG.
[21] J.M. Azzi, S. Tahiri, A. Albizane, A. Messaoudi, M. Bouhria, S. Alami Younssi, A. Mourid, Amrhar, Study of quality of a pigment prepared by complexation of chromates recovered from treated chrome shavings and tanned splits, J. Am. Leather Chem. Assoc. 96 (2001) 426–436.
[22] S. Selvaraj, S. Ramalingam, S. Parida, J.R. Rao, N.F. Nishter, Chromium containing leather trimmings valorization: Sustainable sound absorber from collagen hydrolysate intercalated electrospun nanofibers, J. Hazard. Mater. 405 (June 2020) (2021) 124231, https://doi.org/10.1016/j.jhazmat.2020.124231.
[23] N. Konikkara, N. Punithavelan, L.J. Kennedy, J.J. Vijaya, A new approach to solid waste management: fabrication of supercapacitor electrodes from solid leather wastes using aqueous KOH electrolyte, Clean Techn. Environ. Policy 19 (4) (2017) 1087–1098, https://doi.org/10.1007/s10098-016-1301-1.
[24] Z. Yang, H. Peng, W. Wang, T. Liu, Crystallization behavior of poly (ε-caprolactone)/layered double hydroxide nanocomposites, J. Appl. Polym. Sci. 116 (5) (2010) 2658–2667, https://doi.org/10.1002/app.
[25] C. Li, et al., The fabrication of thermoplastic polyurethane/leather powder composite film with excellent mechanical property, Composites Communications 25 (March) (2021) 100694, https://doi.org/10.1016/j.coco.2021.100694.
[26] P. Thanikaivelan, N.T. Narayanan, B.K. Pradhan, P.M. Ajayan, Collagen based magnetic nanocomposites for oil removal applications, Sci. Rep. 2 (2012), https://doi.org/10.1038/srep00230.
[27] R.D. Kale, N.C. Jadhav, Utilization of waste leather for the fabrication of composites and to study its mechanical and thermal properties, SN Appl. Sci. 1 (10) (2019) 1–9, https://doi.org/10.1007/s42452-019-1230-9.
[28] E. Kiliç, Q. Tarrés, M. Delgado-Aguilar, X. Espinach, P. Fullana-I-palmer, R. Puig, Leather waste to enhance mechanical performance of high-density polyethylene, Polymers (Basel) 12 (9) (2020) 1–15, https://doi.org/10.3390/polym12092016.
[29] M.R. Ruiz, P.L.S. Cabreira, E.R. Budemberg, E.A.P. Dos Reis, F.S. Bellucci, A.E. Job, Chemical evaluation of composites natural rubber/carbon black/leather tannery projected to antistatic flooring, J. Appl. Polym. Sci. 133 (27) (2016) 1–10, https://doi.org/10.1002/app.43618.
[30] D.G.S.M. Cavalcante, et al., Composites produced from natural rubber and chrome-tanned leather wastes: evaluation of their in vitro toxicological effects for application in footwear and textile industries, J. Polym. Environ. 26 (3) (2018) 980–988, https://doi.org/10.1007/s10924-017-1002-9.
[31] W. Urrego Yepes, N. Cardona, S.M. Velasquez, D.H. Giraldo Vásquez, J.C. Posada, Mechanical and rheometric properties of natural rubber composites filled with untreated and chemically treated leather wastes, J. Compos. Mater. 53 (11) (2019) 1475–1487, https://doi.org/10.1177/0021998318805195.
[32] L.T. Hang, et al., Utilization of leather waste fibers in polymer matrix composites based on acrylonitrile-butadiene rubber, Polymers (Basel) 13 (1) (2021) 1–11, https://doi.org/10.3390/polym13010117.
[33] S. Talib, A.Z. Romli, S.Z. Saad, The effect of filler loading on the flexural and compressive properties of untreated and treated chrome tanned leather waste (CTLW) short fibre filled unsaturated polyester composites, AIP Conf. Proc. 1985 (2018), https://doi.org/10.1063/1.5047165.
[34] Y. Liu, Q. Wang, L. Li, Reuse of leather shavings as a reinforcing filler for poly (vinyl alcohol), J. Thermoplast. Compos. Mater. 29 (3) (2016) 327–343, https://doi.org/10.1177/0892705713518794.
[35] T. Ambone, S. Joseph, E. Deenadayalan, S. Mishra, S. Jaisankar, P. Saravanan, Polylactic acid (PLA) biocomposites filled with waste leather buff (WLB), J. Polym. Environ. 25 (4) (2017) 1099–1109, https://doi.org/10.1007/s10924-016-0891-3.
[36] S. Li, Y. Wang, W. Xu, B. Shi, Natural rubber-based elastomer reinforced by chemically modified multiscale leather collagen fibers with excellent toughness, ACS Sustain. Chem. Eng. 8 (13) (2020) 5091–5099, https://doi.org/10.1021/acssuschemeng.9b07078.
[37] K. Chronska, A. Przepiorkowska, Buffing dust as a filler of carboxylated butadiene-acrylonitrile rubber and butadiene-acrylonitrile rubber, J. Hazard. Mater. 151 (2–3) (2008) 348–355, https://doi.org/10.1016/j.jhazmat.2007.05.087.
[38] G. Scetta, N. Selles, P. Heuillet, M. Ciccotti, C. Creton, Cyclic fatigue failure of TPU using a crack propagation approach, Polym. Test. 97 (2021) 107140, https://doi.org/10.1016/j.polymertesting.2021.107140.
[39] G. de Avila Bockorny, M.M.C. Forte, S. Stamboroski, M. Noeske, A. Keil, W. L. Cavalcanti, Modifying a thermoplastic polyurethane for improving the bonding performance in an adhesive technical process, Appl. Adhes. Sci. 4 (1) (2016), https://doi.org/10.1186/s40563-016-0060-x.
[40] J. Tan, Y.M. Ding, X.T. He, Y. Liu, Y. An, W.M. Yang, Abrasion resistance of thermoplastic polyurethane materials blended with ethylene–propylene–diene monomer rubber, J. Appl. Polym. Sci. 110 (3) (Nov. 2008) 1851–1857, https://doi.org/10.1002/APP.28756.
[41] B. Liu, Y. Li, Q. Wang, S. Bai, Green fabrication of leather solid waste/thermoplastic polyurethanes composite: physically de-bundling effect of solid-state shear milling on collagen bundles, Compos. Sci. Technol. 181 (June) (2019) 107674, https://doi.org/10.1016/j.compscitech.2019.06.001.
[42] R. Ahmed, W. Wang, A.W. Zia, Collagen Formation Observed from Healing Calvarial Defects with Principal Component Analysis of Raman Scattering, The Royal Society of Chemistry, 2018, pp. 4614–4622, https://doi.org/10.1039/c8an01021h.
[43] M. Mehta, R. Naffa, C. Maidment, G. Holmes, M. Waterland, Raman and Atr-Ftir spectroscopy towards classification of wet blue bovine leather using Ratiometric and Chemometric analysis, J. Leather Sci. Eng. 2 (1) (2020), https://doi.org/10.1186/s42825-019-0017-5.
[44] D. Xu, F. Liu, G. Pan, Z. Zhao, X. Yang, H. Shi, Softening and hardening of thermal plastic polyurethane blends by water absorbed, Polymer (Guildf) 218 (November 2020) (2021) 123498, https://doi.org/10.1016/j.polymer.2021.123498.
[45] M. Aurilia, F. Piscitelli, L. Sorrentino, M. Lavorgna, S. Iannace, Detailed analysis of dynamic mechanical properties of TPU nanocomposite: the role of the interfaces, Eur. Polym. J. 47 (5) (2011) 925–936, https://doi.org/10.1016/j.eurpolymj.2011.01.005.
[46] M. Nofar, E. Büşra Küçük, B. Batı, Effect of hard segment content on the microcellular foaming behavior of TPU using supercritical CO2, J. Supercrit. Fluids 153 (2019), https://doi.org/10.1016/j.supflu.2019.104590.
[47] M. Khalifa, S. Anandhan, G. Wuzella, H. Lammer, A.R. Mahendran, Thermoplastic polyurethane composites reinforced with renewable and sustainable fillers–a review, Polyme.-Plast. Technol. Materi. 59 (16) (2020) 1751–1769, https://doi.org/10.1080/25740881.2020.1768544.
[48] M. Kannan, S.S. Bhagawan, S. Thomas, K. Joseph, Thermogravimetric analysis and differential scanning calorimetric studies on nanoclay-filled TPU/PP blends, J. Therm. Anal. Calorim. 112 (3) (2013) 1231–1244, https://doi.org/10.1007/s10973-012-2693-8.
[49] D. Tabuani, F. Bellucci, A. Terenzi, G. Camino, Flame retarded thermoplastic polyurethane (TPU) for cable jacketing application, Polym. Degrad. Stab. 97 (12) (2012) 2594–2601, https://doi.org/10.1016/j.polymdegradstab.2012.07.011.
[50] A.K.M. Herreraa, G. Matuscheka, Polymer degradation and stability 78 (2002) 323–331 www.elsevier.com/locate/polydegstab thermal degradation of thermoplastic polyurethane elastomers (TPU) based on MDI, Polym. Degrad. Stab. 46 (2) (2002) 323–344.
[51] E. Bañón, A.N. García, A. Marcilla, Thermogravimetric analysis and Py-GC/MS for discrimination of leather from different animal species and tanning processes, J. Anal. Appl. Pyrolysis 159 (September) (2020) 2021, https://doi.org/10.1016/j.jaap.2021.105244.
[52] A. Nanni, M. Parisi, M. Colonna, M. Messori, Thermo-mechanical and morphological properties of polymer composites reinforced by natural fibers derived from wet blue leather wastes: a comparative study, Polymers (Basel) 13 (11) (2021), https://doi.org/10.3390/polym13111837.
[53] J.K. Kanagaraj, R.C. Panda, M.V.K. Vinodh Kumar, Trends and advancements in sustainable leather processing: future directions and challenges-a review, J. Environ. Chem. Eng. 8 (5) (2020) 104379, https://doi.org/10.1016/j.jece.2020.104379.
[54] H. Lakrafli, S. Tahiri, A. Albizane, M.E. El Otmani, Effect of wet blue chrome shaving and buffing dust of leather industry on the thermal conductivity of cement and plaster based materials, Constr. Build. Mater. 30 (2012) 590–596, https://doi.org/10.1016/j.conbuildmat.2011.12.041.
[55] I.S. Czirok, et al., Thermal characterization of leathers tanned by metal salts and vegetable tannins, J. Anal. Appl. Pyrolysis 173 (May) (2023), https://doi.org/10.1016/j.jaap.2023.106035.
[56] N. Konikkara, L.J. Kennedy, J.J. Vijaya, Preparation and characterization of hierarchical porous carbons derived from solid leather waste for supercapacitor applications, J. Hazard. Mater. 318 (2016) 173–185, https://doi.org/10.1016/j.jhazmat.2016.06.037.
[57] Z. Sebestyén, E. Jakab, E. Badea, E. Barta-Rajnai, C. Şendrea, Z. Czégény, Thermal degradation study of vegetable tannins and vegetable tanned leathers, J. Anal. Appl. Pyrolysis 138 (November 2018) (2019) 178–187, https://doi.org/10.1016/j.jaap.2018.12.022.
[58] E.B.A. Marcilla, A.N. García, M. León, P. Martínez, Study of the influence of NaOH treatment on the pyrolysis of different leather tanned using thermogravimetric analysis and Py / GC – MS system, J. Anal. Appl. Pyrolysis 92 (2011) 194–201, https://doi.org/10.1016/j.jaap.2011.05.014.
[59] M. Kirpluks, U. Cabulis, A. Ivdre, M. Kuranska, M. Zieleniewska, M. Auguscik, Mechanical and thermal properties of high-density rigid polyurethane foams from renewable resources, J. Renew. Mater. 4 (1) (2016) 86–100, https://doi.org/10.7569/JRM.2015.634132.
[60] M.M. Hassan, Enhanced antistatic and mechanical properties of corona plasma treated wool fabrics treated with 2,3-epoxypropyltrimethylammonium chloride, Ind. Eng. Chem. Res. 53 (27) (2014) 10954–10964, https://doi.org/10.1021/ie500447p.
[61] C. Lluch, et al., Antimicrobial polyurethane thermosets based on undecylenic acid: synthesis and evaluation, Macromol. Biosci. 14 (8) (2014) 1170–1180, https://doi.org/10.1002/mabi.201400017.
[62] G. Giubertoni, et al., Hydrogen bonds under stress: strain-induced structural changes in polyurethane revealed by rheological two-dimensional infrared spectroscopy, J. Phys. Chem. Lett. 14 (4) (2023) 940–946, https://doi.org/10.1021/acs.jpclett.2c03109.

[63] N. Sasaki, S. Odajima, Stress-strain curve and Young's modulus of a collagen molecule as determined by the X-ray diffraction technique, J. Biomech. 29 (5) (1996) 655–658, https://doi.org/10.1016/0021-9290(95)00110-7.
[64] J.A.J. Van Der Rijt, K.O. Van Der Werf, M.L. Bennink, P.J. Dijkstra, J. Feijen, Micromechanical testing of individual collagen fibrils, Macromol. Biosci. 6 (9) (2006) 697–702, https://doi.org/10.1002/mabi.200600063.
[65] P. Dutov, O. Antipova, S. Varma, J.P.R.O. Orgel, J.D. Schieber, Measurement of elastic modulus of collagen type i single fiber, PLoS One 11 (1) (2016) 1–13, https://doi.org/10.1371/journal.pone.0145711.